NONLINEAR FINITE ELEMENT MODELLING OF TRANSIENT GEOTHERMAL PROCESS IN POROUS MEDIA WITH LIQUID/VAPOR PHASE CHANGE

Ji Zhang[1] and Huilin Xing[1]

[1]Earth Systems Science Computational Centre, School of Earth Sciences, The University of Queensland, St Lucia 4072 Australia

ji.zhang@uq.edu.au, h.xing@uq.edu.au

Keywords: *Phase change, finite element method, coupled problem, Newton-Raphson method, porous media.*

ABSTRACT

A numerical model is developed for simulating liquid/vapor two-phase coupled fluid and heat flow in porous media, particularly towards hydrothermal/geothermal reservoirs. The model is formulated as two nonlinear equations with pressure and enthalpy as the primary variables. Water thermodynamic properties are calculated using IAPWS-IF97, the latest available industrial standard. Their derivatives with respect to pressure and enthalpy are also deduced from the above IF97 steam table functions. All seven material coefficients of the coupled equations show high nonlinearities with severe slope discontinuities at the liquid/vapor phase change. The coupled highly nonlinear equations are solved simultaneously using a Newton-Raphson based nonlinear finite element technique. Different convergence criteria together with a phase change control module and an automatic time step size control module are employed to ensure convergence of the Newtonian iteration under various conditions. The above numerical model is applied to simulate the depressurising process of a coastal deep mining field with a high temperature zone. Numerical results show its potential usefulness in predicting the temperature decrease, pressure relief and steam liberation of a practical geothermal mining field.

1. INTRODUCTION

Non-isothermal flow in porous media is important in several practical areas, such as groundwater remediation techniques, underground mining processes, extraction of geothermal energy, and geotechnical technologies for waste isolation. Numerical modeling is necessary to evaluate the impact of coupling phenomena on overall system performance. Great efforts have been devoted to modeling multi-phase coupled fluid and heat flow in porous media for both immiscible fluid (e.g. the oil-water-air-gas system as shown in Aziz and Settari 1979, Kolditz and De Jonge 2004) and miscible fluid (e.g. those involving single or multiple solvents with single or multiple miscible fluids as shown in Bear 1972, Nield and Bejan 1992). Commonly employed numerical methods for modeling such coupled fluid and heat flow phenomena are the Finite Difference (see e.g. Ozisik and Czisik 1994), Finite Volume (see e.g. Patankar 1980), Finite Element and Boundary Elements (see e.g. Ibanez and Power 2002) techniques.

The liquid/vapor two-phase non-isothermal system with phase change is widely observed but considerably different from the conventional cases above. This is because the two phases under consideration (i.e. liquid water and vapor) not only co-exist in the same volume (miscible), but also exchange mass during the phase change. Mass exchange between two phases with large density ratio ($\approx$1000) makes numerical modeling extremely difficult. In addition, numerical modeling of such problems needs to account for incompressible or slightly compressible (liquid) and compressible (vapor) flows in the same computational domain. In fact, there are few reported simulations of liquid/vapor flows coupled with heat flow accompanied by a phase change with realistic physical properties in the literature. TOUGH2 is a finite difference based numerical simulator which can model liquid/vapor two-phase problems with phase change (Pruess 1991). TOUGH2 treats phase change by a primary variables switching technique (Pruess et al. 1999); i.e. the primary variables are switched from pressure and temperature to pressure and saturation when a phase change occurs. TOUGH2 has been widely used in geothermal industry with a focus on evaluation of long-term potential of steam production for power generation from a specific geothermal reservoir, rather than transient geothermal processes. Most recently, Muhieddine et al. (2011) developed a finite volume method based model to simulate the water forced evaporation in a porous saturated medium. By neglecting pressure variation to make the boiling point temperature constant and using smoothed physical properties, their model was simplified to a set of temperature/pressure formulated partial differential algebraic equations and applied to simulate heat diffusion and water steam flow.

Finite element modeling of two phase flow problem is also found in the literature. Zyvoloski et al. (1999) proposed their Finite Element Heat and Mass transfer code (FEHM) with consideration of liquid vapor phase transition. Lewis et al. (1989) also proposed a finite element approach for solving two phase heat and fluid flow in deforming porous media. In both approaches pressure and temperature are used as the main variables for fluid flow and energy equations. Thus determination of the thermodynamic phase region (e.g. liquid, vapor and mixture) is a prerequisite to calculating thermodynamic properties in these models. Huyakorn and Pinder (1978) showed that this is not necessary when pressure and enthalpy are chosen as the primary variables, as these two variables uniquely define the thermodynamic state of the system and the temperature and phase saturation can be determined a posteriori when the solution is complete. However, in their model, the thermodynamic properties of water are simplified to several regression formulae. Thus far, the numerical/experimental study of liquid/vapor two-phase flow with phase change in geothermal systems remains challenging and is the subject of continuing research.

This paper focuses on simulating the transient process in porous media with phase change by using a finite element method detailed below. The pressure and enthalpy based governing equations and auxiliary assumptions/equations involved in coupled liquid/vapor two phase fluid and heat flow in porous media are formulated using a nonlinear finite element method for solving multidimensional phase change problems. The latest IAPWS Industry Formulation 1997 (IF97) for steam table equations (IAPWS 2007) is used to

describe material properties under various thermodynamic conditions. The detailed nonlinearities and slope discontinuities existing in the coefficients of the equations are investigated, and then several numerical techniques that deal with nonlinearities are proposed. These incluce automatic time step size control and specific numerical techniques used at phase change boundary. The model is applied to analyse pressure, temperature, and water saturation changes under varying production rates of a well in a coastal deep mining field with a high temperature zone.

2. GOVERNING EQUATIONS

Assuming thermal equilibrium exists among the liquid water, vapor and rock matrix, the general mathematical model for describing the conservation of mass and energy of a two-phase reservoir is given by Faust and Mercer (1977):

$$\frac{\partial(\phi S_p \rho_p)}{\partial t} + \nabla \cdot (\rho_p v_p) - q_m = 0 \tag{1}$$

$$\frac{\partial[\phi S_p \rho_p H_p + (1-\phi)\rho_r H_r]}{\partial t} + \nabla \cdot (\rho_p H_p v_p) - \nabla \cdot (\lambda_m \nabla T) - q_e = 0 \tag{2}$$

where ϕ is the porosity; S is the phase saturation; ρ is the density [kg/m^3]; v is the fluid velocity vector [m/s]; H is the specific enthalpy [kJ/kg]; λ_m is the thermal conductivity tensor of the porous medium [W/m·K]; T is temperature [°C]; q_m and q_e are source/sink of the total mass and energy respectively [kg/m^3·s, kJ/m^3·s]. The subscript p denotes the phases; i.e. p=w for liquid, p=s for vapor. Subscript p also implies summation convention over the two phases. The subscript r denotes the rock matrix.

The two-phase Darcy's Law for multiphase flow is used to describe the momentum balance:

$$v_p = -\frac{K k_{rp}}{\mu_p} \cdot (\nabla P_p - \rho_p g \nabla D) \tag{3}$$

where P is fluid pressure [Pa]; K is the intrinsic permeability tensor of the porous medium [m^2], k_r is the relative permeability of the phase; μ is the dynamic viscosity [kg/m·s]; g is gravity [m/s^2], D is the depth [m];

Substituting the momentum equation (3) into the mass and energy conservation Equations (1-2), and using pressure (P) and enthalpy (H) as the primary variables, we obtain the following mathematical equations:

$$\frac{\partial(\phi S_p \rho_p)}{\partial t} - \nabla \cdot \left(\frac{K k_{rp} \rho_p}{\mu_p} \cdot (\nabla P_p - \rho_p g \nabla D)\right) - q_m = 0 \tag{4}$$

$$\frac{\partial[\phi S_p \rho_p H_p + (1-\phi)\rho_r H_r]}{\partial t} - \nabla \cdot \left(\frac{K k_{rp} \rho_p H_p}{\mu_p} \cdot (\nabla P_p - \rho_p g \nabla D)\right) - \nabla \cdot \left(\lambda_m \frac{\partial T}{\partial P} \nabla P_p + \lambda_m \frac{\partial T}{\partial H} \nabla H\right) - q_e = 0 \tag{5}$$

Other auxiliary assumptions and equations are listed as follows.

1. Pressure. The pressure of each phase is equal; i.e. the capillary pressure is assumed negligible: $P_w = P_s$.

2. Enthalpy. The enthalpy of the liquid/vapor mixture is defined as: $H = (\rho_w S_w H_w + \rho_s S_s H_s)/\rho$.

3. Temperature. The temperature and its derivatives with respect to pressure and enthalpy are functions of pressure and enthalpy, which are determined by the fluid thermodynamic property functions.

4. Density and viscosity of the fluid. The density of the liquid/vapor mixture is defined as: $\rho = \rho_w S_w + \rho_s S_s$. The density and viscosity are functions of pressure and enthalpy according to the fluid thermodynamic property functions.

5. Fluid saturation. The volume saturation of each phases sums to 1: $S_w + S_s = 1$. In the pure liquid region, the liquid saturation is assumed to be 1, and in the saturated vapor region, it is assumed to be 0. In the two-phase region, phase saturations are derived and calculated by the density and enthalpy equations, so they are also functions of pressure and enthalpy.

6. Porous media properties. The porosity, intrinsic permeability, rock density and specific heat are functions of spacial coordinates.

7. Rock specific enthalpy is a linear function of temperature, given by $H_r = c_r T$, where c_r is the specific heat of the rock.

8. Relative permeabilities. The relative permeabilities of the liquid and vapor are functions of phase saturation. We employ the following form of relative permeabilities (Huyakorn & Pinder, 1978):

$$k_{rw} = S_w^2, k_{rs} = (1 - S_w)^2 \tag{6}$$

Using pressure and enthalpy as primary variables, and combining the coefficients in Equations (4-5), the governing equations are rewritten in reduced parameter form as:

$$\frac{\partial}{\partial x}\left(\tau \frac{\partial P}{\partial x}\right) = C^P \frac{\partial P}{\partial t} + C^H \frac{\partial H}{\partial t} \tag{7}$$

$$\frac{\partial}{\partial x}\left(\lambda \frac{\partial P}{\partial x}\right) + \frac{\partial}{\partial x}\left(\beta \frac{\partial H}{\partial x}\right) = D^P \frac{\partial P}{\partial t} + D^H \frac{\partial H}{\partial t} \tag{8}$$

in which τ, C^P, C^H, λ, β, D^P, D^H are the seven nonlinear coefficients defined as follows. The source/sink terms in Equations (4-5) have not appeared in Equation (7-8) and are treated as boundary conditions.

$$\tau = \tau_w + \tau_s \tag{9}$$

$$C^P = \phi\left(\frac{\partial \rho}{\partial P}\right)_H \tag{10}$$

$$C^H = \phi\left(\frac{\partial \rho}{\partial H}\right)_P \tag{11}$$

$$\lambda = \begin{cases} \lambda_m\left(\dfrac{\partial T}{\partial P}\right)_H + H_w^{sat}\tau_w + H_s^{sat}\tau_s, \text{ for } H_w^{sat} \le H \le H_s^{sat} \\ \lambda_m\left(\dfrac{\partial T}{\partial P}\right)_H + \tau H, \text{ for } H < H_w^{sat} \text{ or } H > H_s^{sat} \end{cases} \tag{12}$$

$$\beta = \lambda_m \left(\frac{\partial T}{\partial H} \right)_P \tag{13}$$

$$D^P = \phi H \frac{\partial \rho}{\partial P} + (1-\phi)\rho_r c_r \left(\frac{\partial T}{\partial P} \right)_H \tag{14}$$

$$D^H = \phi H \frac{\partial \rho}{\partial H} + \phi\rho + (1-\phi)\rho_r c_r \left(\frac{\partial T}{\partial H} \right)_P \tag{15}$$

where H_w^{sat} and H_s^{sat} are saturated liquid water enthalpy and vapor enthalpy under given pressure, respectively.

The phase mobility is defined as

$$\tau_p = \frac{K k_{rp} \rho_p}{\mu_p} \tag{16}$$

The elevation terms ($\rho_p g \nabla D$) have been neglected for the sake of simplicity because the models in this paper handle only horizontal two dimensional domains. In a three dimensional model, this term cannot be neglected.

3. FLUID THERMODYNAMIC PROPERTIES

As previously mentioned, the fluid thermodynamic properties, such as temperature, density and viscosity, are determined from the fluid thermodynamic property functions, which are a set of so-called Equations-Of-State. The International Association for the Properties of Water and Steam (IAPWS) has taken responsibility for standardizing the thermodynamic properties of water. The updated formulations for several properties are available on the IAPWS web page (http://www.iapws.org/). The fundamental work in developing the regression equations for a wide range of temperatures and pressures is from the late 1960s. Wagner et al. (2000) presented a comprehensive study on the evolution of thermodynamics formulations for the properties of pure water from the first formulation (IFC-68) to the mostly accepted IF97 formulation for scientific use. Figure 1 shows the latest version of regions and equations of IAPWS-IF97, which are valid for the following range: 273.15K $\leqslant T \leqslant$ 1073.15K, $P \leqslant$ 100MPa; and 1073.15K<T≤2273.15K, P≤50MPa (IAPWS 2007). They also conducted a comparative evaluation study of the existing formulations and demonstrated the advantages of IF97 formulation in obtaining consistent values for the thermodynamic properties of water, even near the critical point of water (Wagner et al. 2000; Wagner and Pruß 2002).

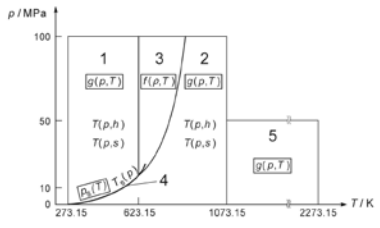

Figure 1: Regions and equations of IAPWS-IF97 (IAPWS 2007)

In this paper a full implementation of IF97 formulation is used to calculate water thermodynamic properties as functions of pressure and enthalpy. The derivatives of the thermodynamic properties with respect to pressure and enthalpy, i.e., $\frac{\partial T}{\partial P}$, $\frac{\partial T}{\partial H}$, $\frac{\partial \rho}{\partial P}$, $\frac{\partial \rho}{\partial H}$, are also developed according to the original IF97 equations. For instance, in region 1 of IAPWS-IF97, which is defined by the temperature and pressure ranges (273.15K$\leqslant T \leqslant$623.15K, Ps(T) $\leqslant P \leqslant$100MPa), the backward equation $T(P,H)$ has the following form:

$$T(P,H) = T^* \sum_{i=1}^{20} n_i \left(\frac{P}{P^*} \right)^{I_i} \left(\frac{H}{H^*} + 1 \right)^{J_i} \tag{17}$$

where T^* =1K, P^* =1MPa, H^* =2500kJ/kg. The coefficient n_i and exponents I_i and J_i are given in Table 6 of the original IF97 document (IAPWS 2007). The derivatives of temperature with respect to pressure and enthalpy can be derived as

$$\frac{\partial T(P,H)}{\partial P} = T^* \sum_{i=1}^{20} \frac{n_i}{P^*} \left(\frac{P}{P^*} \right)^{I_i - 1} \left(\frac{H}{H^*} + 1 \right)^{J_i} \tag{18}$$

$$\frac{\partial T(P,H)}{\partial H} = T^* \sum_{i=1}^{20} \frac{n_i}{H^*} \left(\frac{P}{P^*} \right)^{I_i} \left(\frac{H}{H^*} + 1 \right)^{J_i - 1} \tag{19}$$

4. NUMERICAL PROCEDURES

4.1 Nonlinear parameters

The two variables, P and H, specified as the primary unknowns in Equations (7) and (8) uniquely define the thermodynamic state of the system. Once P and H are known, the nonlinear parameters can be calculated using the prescribed equations together with the fluid thermodynamic property functions. Typical plots of τ , C^P , C^H , λ , β , D^P , D^H are shown in Figure 2. They demonstrate that these functions are highly nonlinear in the two-phase zone of the thermodynamic region. Furthermore, sharp discontinuities exist at the boundary of the two-phase and single-phase zones. These features make the two-phase problem very difficult to solve by conventional numerical methods when liquid and vapor phases coexist, and significant mass exchange between the two phases is occuring.

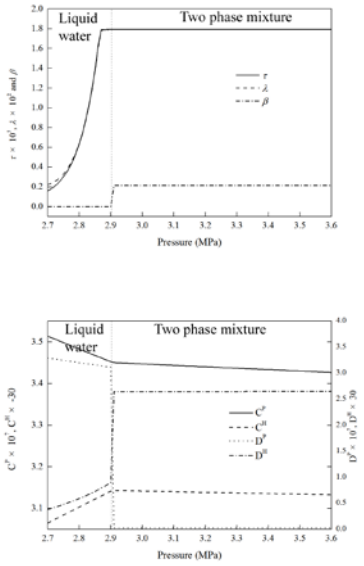

Figure 2: Variation of nonlinear parameters with pressure (H=1000kJ). Left area of the vertical dash line: liquid water zone, right area of the vertical dashed line: two phase mixture zone.

4.2 Solution procedures

The combination of high nonlinearities and slope discontinuities usually results in convergence difficulties and induces severe restrictions on time step size. Furthermore, the hyperbolic character of the two equations often leads to oscillatory behaviour of numerical results. The oscillations are unacceptable because they can become greatly amplified through calculation of the nonlinear parameters, especially on the phase change boundaries. This is the main reason that simulations of liquid/vapor flows coupled with heat flow and phase change with realistic physical properties are uncommon. To overcome these difficulties, we propose a finite element technique in which Equations (7) and (8) are firstly discretized via a general weighted residual formulation in space, and a second-order Crank-Nicolson differencing method in the time domain; then the resulting set of nonlinear algebraic equations is solved by a Newton-Raphson iterative scheme.

A detailed finite element implementation process is proposed in Huyakorn and Pinder (1978). The model in this paper uses a similar derivation, but with a different treatment for the right hand side of the Equations (7) and (8), which result in four nonlinear parameters on the right hand side instead of two. This is for linearization purposes for the Newton-Raphson procedure. Furthermore, the proposed model use a second-order Crank-Nicholson differencing method for the temporal discretization instead of the explicit method introduced in Huyakorn and Pinder (1978) , which improves the accuracy of the solution. The thermodynamic properties of water are calculated by the IF97 formulation instead of simplified regression formulae. Model validation is reported in Xing et al. (2008) and Bringemeier et al. (2010). The final equation of the Newton-Raphson iteration can be derived as:

$$[A]\begin{Bmatrix}\Delta P\\ \Delta H\end{Bmatrix}=\begin{Bmatrix}-R_m^k\\ -R_e^k\end{Bmatrix} \tag{20}$$

where the stiffness matrix

$$[A]=\begin{bmatrix}\dfrac{\partial R_m}{\partial P_J} & \dfrac{\partial R_m}{\partial H_J}\\ \dfrac{\partial R_e}{\partial P_J} & \dfrac{\partial R_e}{\partial H_J}\end{bmatrix} \tag{21}$$

and the residuals

$$R_m=\int_V\left[\frac{W_I}{\Delta t}C^P+\frac{\partial W_I}{\partial x_i}\theta\tau\frac{\partial N_J}{\partial x_i}\right]\Delta P_J\mathrm{d}V+\int_V\frac{W_I}{\Delta t}C^H\Delta H_J\mathrm{d}V+\int_V\frac{\partial W_I}{\partial x_i}\tau\frac{\partial N_J}{\partial x_i}P_J^t\mathrm{d}V-\int_V W_I q_m\mathrm{d}V \tag{22}$$

$$R_e=\int_V\left[\frac{W_I}{\Delta t}D^P+\frac{\partial W_I}{\partial x_i}\theta\lambda\frac{\partial N_J}{\partial x_i}\right]\Delta P_J\mathrm{d}V+\int_V\left[\frac{W_I}{\Delta t}D^H+\frac{\partial W_I}{\partial x_i}\theta\beta\frac{\partial N_J}{\partial x_i}\right]\Delta H_J\mathrm{d}V+\int_V\frac{\partial W_I}{\partial x_i}\lambda\frac{\partial N_J}{\partial x_i}P_J^t\mathrm{d}V+\int_V\frac{\partial W_I}{\partial x_i}\beta\frac{\partial N_J}{\partial x_i}H_J^t\mathrm{d}V-\int_V W_I q_e\mathrm{d}V \tag{23}$$

and the derivatives of the residuals $\frac{\partial R_m}{\partial P_J}$, $\frac{\partial R_m}{\partial H_J}$, $\frac{\partial R_e}{\partial P_J}$, $\frac{\partial R_e}{\partial H_J}$ can be derived from Equations (22) and (23). N_J and W_I are the basic shape functions and weighting functions (Huyakorn and Pinder, 1978). θ is the implicitness factor of the Crank-Nicholson scheme, $0<\theta<1$. Δt is the time step size and ΔP and ΔH are pressure and enthalpy increments. The superscript *t* denotes the value from last time step.

To calculate the nonlinear parameters' derivatives with respect to pressure and enthalpy analytically, we consider not only the original parameter equations (i.e., Equations (11-17)), but also the secondary variables and their derivatives, such as S_w, $\frac{\partial S_w}{\partial P}$, $\frac{\partial S_w}{\partial H}$, k_{rw}, $\frac{\partial k_{rw}}{\partial P}$, $\frac{\partial k_{rw}}{\partial H}$, k_{rs}, $\frac{\partial k_{rs}}{\partial P}$, $\frac{\partial k_{rs}}{\partial H}$. These algebraic derivation processes are treated carefully as they can introduce additional discontinuities to the final equations if their first derivatives with respect to pressure and enthalpy have slope discontinuities.

4.3 Automatic time step size control

Automatic time step control is essential for strongly nonlinear coupled equations. In this paper, the nonlinearity of the equations is severe and the parameters change rapidly at the phase change boundaries (Figure 2). Small time steps are required for a stable computation and an accurate solution when the parameters change rapidly at phase change. To control the time step size at the moment of phase change, a simple but efficient algorithm is applied when phase change occurs. As shown in Figure 3, a relatively large time step size is used at the beginning of the simulation. If phase change takes place in certain time step, the proposed algorithm determines the number of phase change nodes (*pc*). If *pc* is greater than a threshold number of phase change nodes per time step ($pc_{\max}$), the time step size has to be cut by a factor of α ($0<\alpha<1$). The multiplier α is determined by the max value between 0.5 and $pc_{\max}/pc$, which means the updated time step size is always greater or equal to 50% of the current time step size. The current time step is calculated with the updated time step size in a loop until the number of phase change nodes is equal or below the given limit.

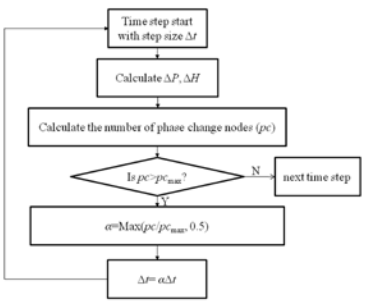

Figure 3: Automatic time step size control algorithm

4.4 Convergence control and phase change control

Equation (20) is solved by the mentioned iterative procedures to convergence. Three criteria are applied to determine convergence of the proposed Newton-Raphson algorithm. The primary convergence criterion is that the infinity norms of the fluid mass residual rates and the energy residual rates for all the nodes are less than a given limits. Nodes with specified pressure and enthalpy boundary conditions are not included in the convergence test because their residuals do not decrease as the solution is approached. Their residuals determine the flow rates through the regional boundary faces.

If phase change occurs in the current time step and three iteration steps have been taken, the secondary convergence criterion is applied. This requires that the infinity norms of the relative changes in pressure and enthalpy over an iteration are less than given limits.

If phase change occurs in the current time step and four iteration steps have been taken, the third convergence criterion is applied, which is that the infinity norm of the absolute change in pressure is less than 1 kPa and the infinity norm of the absolute change in enthalpy is less than 0.01kJ/kg. This criterion is used in the circumstances that the Newton-Raphson algorithm has become stable despite the residual rates exceeding the given tolerance.

A phase change control module is used to help with convergence. For any nodes which have changed phase state during the iteration, the pressure and enthalpy are adjusted mandatorily to near the phase boundary. As shown in Figure 4, assuming the old pressure and enthalpy are (P_0, H_0) and the newly calculated pressure and enthalpy are (P_1, H_1), the phase change control module employs the following algorithm:

i. Calculate the pressure step increment δP and δH by dividing the pressure and enthalpy increment (i.e., P_1-P_0, H_1-H_0) by 100, i.e., δP= (P_1-P_0)/100 and δH= (H_1-H_0)/100;

ii. Let P_2= P_0 and H_2= H_0;

iii Repeat step iv-v until the loop terminates;

iv. P_2= P_2+ δP, H_2= H_2+ δH;

v. For the first iteration, if phase state at (P_2, H_2) is different with that of (P_0, H_0), terminate the loop; for the second and the third iterations, if phase state at (P_2, H_2) is different with that of (P_0, H_0), P_2= P_2- δP, H_2= H_2- δH, terminate the loop;

vi. (P_2, H_2) are the modified pressure and enthalpy for the phase change node after applying the phase change control module.

The proposed algorithm with mandatory adjustment of pressure and enthalpy is to slow the phase change process and avoid irrational jumps of pressure and enthalpy during the phase change. It is implemented in the current finite element model and is useful for avoiding the convergence issues for solving nonlinear coupled heat and fluid flow equations with phase change. Its impact on the entire solution set is minor as it is only applied to very limited number of nodes with phase change and it does not include any mandatory convergence control.

These convergence criteria are applied together with the phase change and time step size control modules to find a stable solution with acceptable accuracy for a given time step under a wide variety of pressure, enthalpy, temperature and phase conditions.

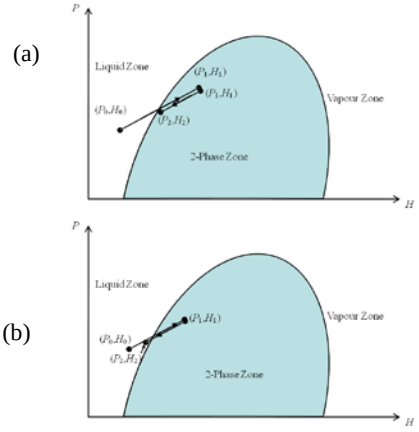

Figure 4: Schematic diagram of the phase change control module for (a) The first iteration; (b) The second and the third iterations.

5. NUMERICAL EXAMPLE

Pump wells, geothermal discharge wells, and pressure relief wells are often employed in underground deep mining to ensure a dry pit and prevent inflows of high temperature geothermal fluids and steam outbursts. Here we develop a hypothetical model to study the temperature decrease, pressure relief and steam liberation in a coastal underground mining field with a high temperature zone. Figure 5 shows the model outline and the initial temperature distribution in the study region. The initial pressure is assumed to be 3.6 MPa throughout the model domain. The seawall is located on the east boundary with constant pressure of 3.6MPa and temperature of 30°C. Due to the existence of the high temperature zone located at the left bottom corner ($r \leqslant 100$m, $r = \sqrt{x^2 + y^2}$), the initial temperature field is not uniform and is defined:

$$T = \begin{cases} 240, & r \le 100 \\ 240 - 160\left(\dfrac{r-100}{200}\right)^2 + 80\left(\dfrac{r-100}{200}\right)^4, & 100 < r \le 300 \\ 160 - 130\dfrac{r-300}{200}, & 300 < r \le 500 \\ 30, & r > 500 \end{cases} \quad (24)$$

Under initial pressure and temperature conditions, the entire region is saturated with liquid water as the boiling temperature of water at 3.6 MPa is 244.2°C. A production well located at (62.5, 62.5) is planned for pressure release and steam liberation before the mining process. Four different well production rate scenarios are analysed to study the well production scenarios: 0.5kg/s, 0.6kg/s, 0.7kg/s and 0.8kg/s.

Each scenario is simulated approximately 12 days after production commences. Parameters used in the simulation are listed in Table 1. Relative permeabilities are given by Equation (6). The region is discretized into a 40×40 rectangle mesh; the minimum time step size for the

simulation is 3×10^4 seconds; the maximum number of phase change nodes per time step is 5.

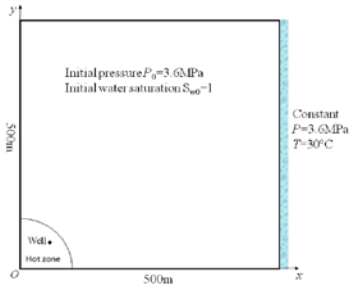

Figure 5: A coastal underground deep mining field with a high temperature zone.

Table 1: Simulation parameters for the coastal underground deep mining field with a geothermal hot zone

Parameter	Value
Reservoir permeability	$1\times10^{-12}m^2$
Reservoir porosity	0.3
Rock thermal conductivity	1.0 W/(m·°C)
Rock heat capacity	1.0 kJ/(kg·°C)
Rock density	2500 kg/m^3
Initial pressure	3.6 MPa
Initial water saturation	1.0

Figure 6 shows variations of water saturation (S_w), pressure (P), enthalpy (H) and temperature (T) at the production well for the four different production rates.

As shown in Figure 6a, for a production rate of 0.5kg/s, no phase change occures and the water remains in the liquid state (S_w=1) during the well production. This is because the production rate is too small to cause a sufficient pressure drop for vaporization. In the other production scenarios vaporization occurs immediately after well production (S_w<1). The lowest water saturations (marked by diamonds) are 0.753, 0.652 and 0.534 at 0.81, 2.43 and 2.66 days, respectively. As production continues, the high temperature zone temperature decreases, which terminates the vaporization process. It takes 3.70, 5.55 and 6.13 days for total liberation of steam (marked by stars), respectively.

Figure 6b shows pressure evolution at the production well for the four scenarios. The pressures drop quickly at the beginning of the production and reach stable values after a period of production. For the production rate of 0.5kg/s, the pressure stabilizes in less than 1 day to 3.36MPa. For the scenarios with phase change (i.e. q=0.6, 0.7 and 0.8kg/s), the pressures stabilize at the end of the vaporization (the star marks), and reach 3.31, 3.26 and 3.21MPa, respectively.

Figure 6c shows enthalpy evolution at the production well for the four scenarios. Due to the non-uniform temperature field of the domain and nonlinear thermodynamic properties, the enthalpy changes are not linear even for the case without phase change (q=0.5 kg/s). For the three cases with phase change, the enthalpies rise with the phase change, and reach a maximum value when the water saturation reaches a minimum value (the diamond marks), then start to decrease rapidly. After vaporization the rate of decrease in enthalpy slows and maintains constant rates.

Figure 6d shows temperature evolution at the production well for the four scenarios. For the scenarios with phase change, the temperature drops rapidly at first and then stay nearly constant after the water saturation reaches a minimum value (the diamond marks), and then drops linearly after vaporization ends (the star marks).

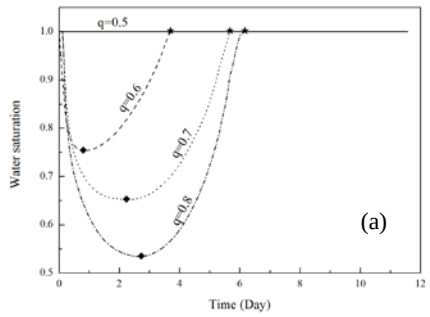

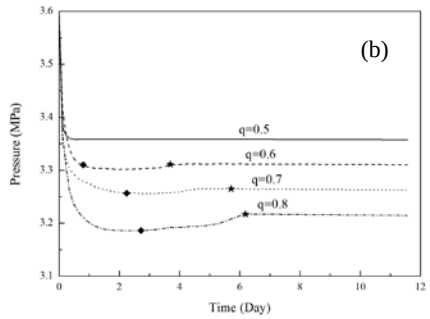

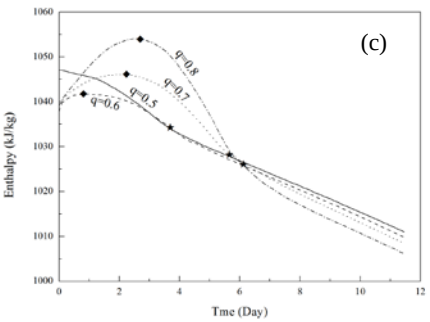

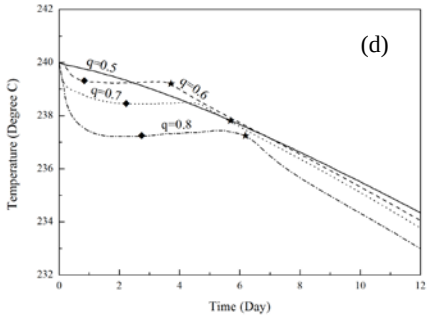

Figure 6: Evolutions of water saturation (a), pressure (b), enthalpy (c) and temperature (d) at the production well for four different production rates (unit of q: kg/s). Diamonds (◆) mark the lowest water saturation points; stars (★) mark the ending points of vaporization.

Figure 7 shows pressure, temperature and water saturation fields of the phase change scenarios (i.e. q=0.6, 0.7 and 0.8kg/s) when water saturation at the well reaches its minimum value (diamond points of Figure 6). The pressure of the hot zone decreases significantly (Figure 7a, d and g). The temperature also decreases in this area (Figure 7b, e and h). The pressure decrease lowers the boiling temperature below the local temperature, which causes phase changes in this area. The water saturation decreases to 0.694 and 0.663 at the left bottom of the domain for q=0.7 and 0.8kg/s, respectively (Figure 7f and i).

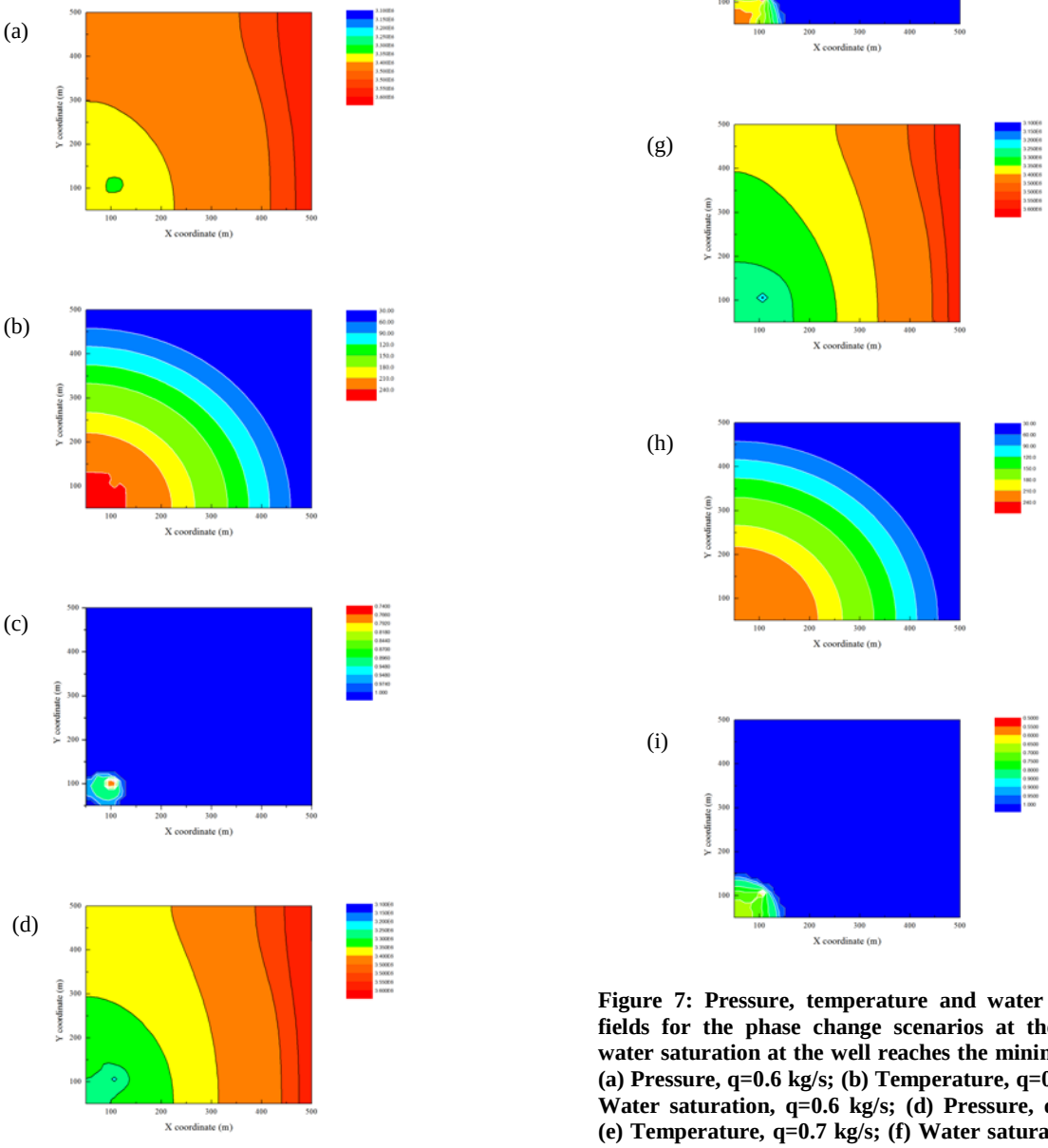

Figure 7: Pressure, temperature and water saturation fields for the phase change scenarios at the time the water saturation at the well reaches the minimum value. (a) Pressure, q=0.6 kg/s; (b) Temperature, q=0.6 kg/s; (c) Water saturation, q=0.6 kg/s; (d) Pressure, q=0.7 kg/s; (e) Temperature, q=0.7 kg/s; (f) Water saturation, q=0.7 kg/s; (g) Pressure, q=0.8 kg/s; (h) Temperature, q=0.8 kg/s; (i) Water saturation, q=0.8 kg/s. Pressure unit: Pa, temperature unit: °C.

6. CONCLUSION

A finite element model is developed for simulation of liquid/vapor two-phase coupled fluid and heat flow in porous media with phase change. The governing equations are formulated in terms of the dependent variables pressure and enthalpy as these two variables uniquely define the thermodynamic state of the system. Water thermodynamic properties are calculated with IAPWS-IF97; their derivatives with respect to pressure and enthalpy are derived from the original IF97 functions. High nonlinearities and severe slope discontinuities exist in the seven coefficients of the governing partial differential equations and make it difficult to solve, especially with phase changes. A Newton-Raphson method is employed to solve the highly nonlinear coupled equations. Three convergence criteria, a phase change control module and an automatic time step size control module are employed to ensure the convergence of the Newton-Raphson iteration.

The model is applied to simulate the temperature decrease, pressure relief and steam liberation of a coastal underground deep mining field with a high temperature zone. The results demonstrate that the pressure and temperature are reduced by the pressure relief well at the high temperature zone. By applying different production rates, the pressure decreases nonlinearly, while temperature decrease is not significantly different except during the early stages of phase change. Different total steam liberation time is also observed under different production rates.

ACKNOWLEDGEMENTS

The authors are grateful to Dr Doone Wyborn of Geodynamics Limited and Professor Hans Muhlhaus of the University of Queensland for their helpful discussions and advices in the relevant research.

REFERENCES

Aziz, K. and Settari, A.: Petroleum reservoir simulation. Applied Science Publishers, London. (1979).

Bear, J.: Dynamics of Fluids in Porous Media. Elsevier, New York. (1972).

Faust, C.R. and Mercer, J.W.: Finite-difference model of two-dimensional single- and two-phase heat transport in a porous medium, version I. Open File Rep.: 77-234, 84 pp., U.S. Geol. Surv., Reston, Va. (1977).

Huyakorn, P. and Pinder, G.F.: A Pressure-Enthalpy Finite Element Model for Simulating Hydrothermal Reservoirs. Mathematics and Computers in Simulation XX: 167-178. (1978).

IAPWS: Revised Release on the IAPWS Industrial Formulation 1997 for the Thermodynamic Properties of Water and Steam. The International Association for the Properties of Water and Steam (IAPWS), Lucerne, Switzerland. (2007).

Ibanez, M.T. and Power, H.: Advanced Boundary Elements for Heat Transfer (Topics in Engineering), WIT Press. (2002).

Kipp, K.L. Jr., Hsieh, P.A., Charlton S.R.: Guide to the revised ground-water flow and heat transport simulator: HYDROTHERM - Version 3: U.S. Geological Survey Techniques and Methods 6−A25: 160. (2008).

Kolditz, O. and De, Jonge J.: Non-isothermal two phase flow in low-permeable porous media. Computational Mechanics 33: 345-364. (2004).

Lewis, R. W., Roberts, P. J., Schrefler, B. A.: Finite element modeling of two-phase heat and fluid flow in deforming porous media, Transport in Porous Media, 4, 319-334, (1989).

Muhieddine, M., Canot1 R., March, Delannay, R.: Coupling heat conduction and water–steam flow in a saturated porous medium. International Journal for Numerical Methods in Engineering 85: 1390–1414. (2011).

Nield, D.A. and Bejan, A.: Convection in Porous Media. Springer Verlag, Berlin. (1992).

Ozisik, M.N. and Czisik, M.N.: Finite Difference Methods in Heat Transfer. CRC Press. (1994).

Patankar, S.V.: Numerical Heat Transfer and Fluid Flow. Hemisphere Publishers. (1980).

Pruess, K.: TOUGH2—a general purpose numerical simulator for multiphase fluid and heat flow. Lawrence Berkeley National Laboratory Report LBL-29400. (1991).

Pruess, K., Oldenburg, C., Moridis, G.: TOUGH2 USER'S GUIDE, VERSION 2.0. Earth Sciences Division, Lawrence Berkeley National Laboratory University of California, Berkeley, California: 30-32. (1999).

Schenk, O. and Gartner, K.: On fast factorization pivoting methods for symmetric indefinite systems. Elec. Trans. Numer. Anal 23:158-179. (2006).

Thomas, L.K., and Pierson, R.G.: Three dimensional reservoir simulation, SPEJ 18: 151-161. (1978).

Wagner, W. and Pruß A.: The IAPWS Formulation 1995 for the Thermodynamic Properties of Ordinary Water Substance for General and Scientific Use, J. Phys. Chem. Ref. Data 31: 387-535. (2002).

Wagner, W., Cooper, J.R., Dittmann, A., Kijima, J., Kretzschmar, H.J., Kruse, A., Mareš, R., Oguchi, K., Sato, H., Stöcker, I., Šifner, O., Takaishi, Y., Tanishita, I., Trübenbach, J., Willkommen, Th.: The IAPWS Industrial Formulation 1997 for the Thermodynamic Properties of Water and Steam, J. Eng. Gas Turbines & Power 122: 150-182. (2000).

Zyvoloski, G.A., Robinson, B.A., Dash, Z.V., Trease L.L.: Models and methods summary for the FEHM application. Los Alamos National Laboratory. (1999).

Xing, H.L.: Progress Report: Supercomputer Simulation of Hot Fractured Rock Geothermal Reservoir Systems: ESSCC/ACcESS Technical Report, The University of Queensland, p.1-48. (2008).

Bringemeier, D., Wang, X.Y., Xing, H.L., Zhang, J.: Modeling of multiphase fluid flow for an open-cut mine development within a Geothermal Active Caldera. In: Proceedings International Association for Engineering Geology and the Environment Congress, Auckland, New Zealand. (2010)